---

**Proceedings Paper:**
Henthorn, S., Mohammadkhani, R., O'Farrell, T. orcid.org/0000-0002-7870-4097 et al. (1 more author) (2022) The effect of ADC resolution on concurrent, multiband, direct RF sampling receivers. In: 2021 IEEE Global Communications Conference, GLOBECOM 2021 - Proceedings. IEEE Global Communications Conference (GLOBECOM), 07-11 Dec 2021, Madrid, Spain. Institute of Electrical and Electronics Engineers . ISBN 9781728181059

https://doi.org/10.1109/GLOBECOM46510.2021.9685641

---

# The effect of ADC resolution on concurrent, multiband, direct RF sampling receivers

Stephen Henthorn, Reza Mohammadkhani, Timothy O'Farrell, and Kenneth Lee Ford
Department of Electronic and Electrical Engineering, University of Sheffield, Sheffield, UK
t.ofarrell@sheffield.ac.uk

***Abstract*—Connectivity using interband frequencies in 4G and 5G radio access networks, for example, carrier aggregation or dual-connectivity, incurs high receiver complexity and power consumption, in particular, when implemented using multiple radio units. Employing concurrent, multiband, direct RF sampling in a single radio chain architecture reduces the RF component count, leading to lower receiver complexity and power consumption. For this architecture, as the composite signal from multiple concurrent bands is digitized by a common analogue-to-digital converter (ADC), the bit resolution critically affects system performance. In this paper, the effect of ADC resolution on the error vector magnitude (EVM) and Block Error Rate (BLER) performance of a concurrent, multiband, direct RF sampling receiver is investigated. Simulation and hardware measurement of a tri-band Long Term Evolution (LTE) system supporting three simultaneously active channels at 888 MHz, 1.92 GHz and 2.52 GHz is evaluated when reducing the ADC resolution from 8 to 3 bits. Interband interference measurements demonstrate that the multiband, direct RF sampling, wideband LTE receiver remains 3GPP compliant at 4-bit ADC resolution with the signal-to-noise-ratio (SNR) desensitization over a single-band receiver limited to 9 dB in the 888 MHz band.**

***Index Terms*—Direct RF sampling; ADC performance; software defined radio; multiband radio receivers; LTE; 5G.**

## I. Introduction

The paper addresses the use of multiple sub-6GHz frequency bands in 4G and 5G radio access networks (RANs) for applications requiring, for example, non-contiguous carrier aggregation or dual-connectivity as encountered in heterogeneous networks (HetNets) [1]. In particular, a concurrent, multiband, direct RF sampling software defined radio (SDR) receiver is investigated with reduced radio frequency (RF) component count obtained by replacing certain RF functionality by digital signal processing (DSP). This, in turn, reduces the cost, complexity and power consumption of the receiver. The direct RF sampling approach considered is based on a single analogue-to-digital converter (ADC) to sample and digitize at Nyquist rates a composite RF signal consisting of multiple wideband LTE signals. Such a concurrent, multiband, direct RF sampling approach using a low bit resolution ADC has not been investigated in the open literature and, in particular, for mobile broadband applications.

The conventional approach for realising concurrent, multiband RF receivers, for mobile broadband applications, is to use an individual RF receiver for each carrier frequency. For example, [2] reports a single-chip device capable of receiving up to three carriers simultaneously using two reconfigurable RF front-ends with separate downconverters and three baseband paths each containing channel select filters and ADCs. The approach, while conceptually straightforward, is complex to implement, has high power consumption and is limited in scale. Single-chip receiver designs aimed at mitigating these drawbacks have been developed. In [3] passive mixing and reconfigurable transimpedance amplifiers are introduced to enhance frequency selectivity whereas in [4] current-efficient, highly linear low noise amplifiers (LNAs) are used to reduce power consumption. However, all of these designs use frequency down conversion, which introduce intermediate frequency (IF) impairments, and a high bit resolution ADC per baseband path.

Another approach to reduce the cost, complexity and power consumption of multiband receivers is to use direct RF subsampling, which employs a single ADC to sample and digitize the composite, multiband RF signal [5]. In subsampling, the least sampling rate is determined by the aggregate bandwidth of the component channels, which typically is considerably less than the lowest RF carrier frequency used [6]. This has the advantage of limiting the power consumption of the ADC, which is known to increase linearly with sampling rate [7]. Recent work has considered the concurrent reception of multiple narrowband signals in GNSS (global navigation satellite system) receivers. In [8], the authors designed a reconfigurable, dual-band, multistandard RF subsampling GNSS receiver whereas in [9] a direct RF subsampling receiver using a common subsampling IF is designed by exploiting the decorrelation of the GNSS spreading codes. However, direct RF subsampling still requires the ADC to respond to the system full RF bandwidth while the procedure to select appropriate subsampling IFs for wideband channels is not readily computable. Also, the theory of noise folding in multiband, direct RF subsampling receivers is incomplete, which can lead to unexpected high signal-to-noise-ratio (SNR) desensitization in certain multiband configurations.

Unlike subsampling, direct RF sampling in multiband receivers does not fold the spectra of signals and noise, thereby avoiding interband interference and SNR degradation. Direct RF sampling at Nyquist rates requires high digitization rates, which increases the power consumption in ADCs. Reducing the power consumption in high sample rate ADCs is an active research area as reviewed in [10]. However, a primary issues for concurrent, multiband, direct RF sampling is SNR desensitization when quantizing a weak signal from one band

in the presence of stronger signals from other bands, which conventionally is resolved by using high bit resolution ADCs. Since ADC power consumption increases exponentially with bit resolution [7], this conventional approach to increasing dynamic range by increasing ADC resolution is extremely limited in multiband direct RF sampling receivers. The authors' work in [11] is the first to address SNR desensitization in multiband direct RF sampling receivers.

Specifically, in [11] the authors experimentally investigated SNR desensitization in a tri-band, direct RF sampling LTE receiver. The architecture of the receiver, which is reproduced in Fig. 1, employed a Nyquist sampling rate of 10 GSample/s and a fixed ADC resolution of 8 bits. The study found that the receiver was desensitized by 3 dB when recovering data from the 888 MHz band with -50 dBm LTE signals in the other two bands, which is 11 dB less than the maximum SNR desensitization permitted by 3GPP specifications [12]. In this paper, the authors are the first to address the issue of reducing ADC power consumption in a tri-band, direct RF sampling receiver by reducing the ADC resolution from 8 to 3 bits as a new design degree of freedom, thereby trading power consumption with tollerable SNR desensitization.

In Section II the receiver architecture is introduced, while its implementation in both an experimental testbed and a Simulink simulation is discussed in Section III. Comprehensive experimental measurements of error vector magnitude (EVM) and block error rate (BLER) in a tri-band, direct RF sampling LTE receiver testbed are presented in Section IV found that a minimum ADC resolution of 4 bits is necessary and sufficient for the receiver SNR desensitization to remain 3GPP compliant when receiving three carriers simultaneously. The measured results are verified by computer simulation of the system in the same Section. Finally, conclusions are drawn in Section V.

## II. Concurrent, tri-band direct RF sampling receiver architecture

Fig. 1 shows the overall architecture of the concurrent tri-band direct RF sampling receiver, which was first introduced in [11]. In keeping with the principles of a software defined radio (SDR), the approach digitizes the signal as soon as possible in order to make the receiver flexible and compact, such as by removing the need for separate downconverter RF circuits for each band. The receiver consists of an RF front-end, performing filtering and amplification of up to three signals in different bands simultaneously; and a digital back-end, where the signals are digitized by a single ADC. The whole digitized signal is presented to three separate SDR receivers, each consisting of a digital downconverter (DDC) centred at the appropriate carrier frequency and baseband (BB) signal processing to retrieve the transmitted data. The error performance in each band depends on the RF front-end, which determines the SNR at the input to the ADC, and the digital processes, particularly the ADC, which introduce further noise into the received waveform. In particular, the effect of the digital processes on performance is under examination in the paper, but first the RF front-end used is described.

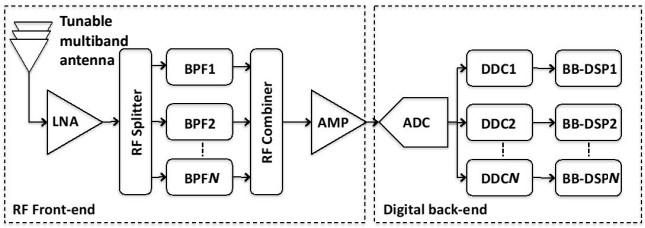


Fig. 1: Tri-band direct RF sampling receiver architecture.

The broadband signals under investigation in this work are at three distinct carrier frequencies: 888 MHz, 1.92 GHz and 2.52 GHz. These were chosen for measurement purposes, but three different LTE compliant bands could also be used. The RF front-end must amplify and filter these signals while adding as little noise and distortion as possible, though it should be noted that the front-end is standards agnostic. In the authors' previous work [11], the first component of the receiver was a tunable tri-band antenna [13], which passes wanted bands while blocking unwanted ones. This work focuses on the effect of the digital back-end, hence, the over-the-air section of the testbed is replaced by cable connections, with the first component being a Mini-circuits ZX60-83LN12+ LNA to provide amplification of the received signal. This provides 21 dB gain between 0.5 GHz and 8 GHz with a noise figure (NF) of 1.4 dB and third order intermodulation product (IP3) of +35.2 dBm, suggesting it is able to amplify the three RF signals concurrently without adding notable distortion.

In order to filter the three bands, the amplified signal is split into three paths and presented to three different static bandpass filters (BPFs) before being recombined. This allows the use of surface acoustic wave (SAW) filters, which provide large out-of-band rejection. Mini-circuits ZN4PD1-63HP-S+ 5-port devices are used as the RF splitter and combiner, with its fourth unused input port terminated with a 50 $\Omega$ load to minimize reflections. These operate between 250 MHz and 6 GHz with insertion loss of 1 dB, isolation of 24 dB and imbalance of 0.2 dB in magnitude and $2^o$ in phase, which ensures the three RF signals are not distorted significantly by the splitting or combining processes. The splitters are rated up to 2 W RF power, which is considerably above the expected combined power of the three signals. TAI-SAW Technology Co. Ltd devices are used for bandpass filtering, specifically TA1889A, TA2018A, and TA1683A. These have centre frequencies of 888.75 MHz, 1.90 GHz and 2.53 GHz, respectively; bandwidths of 17.5 MHz, 40 MHz and 20 MHz, respectively; and nominal insertion losses of 1.4 dB, 1.3 dB and 1.3 dB, respectively. The bandwidths of these commercially available filters cover the typical bands used for LTE and 5G NR standards. For all three filters the stop-band rejection losses are greater than 40 dB. As such, these SAW filters can be expected to provide the filtering required to minimize the effect of out-of-band signals and noise on the receiver, which

may desensitize the ADC.

The disadvantage of this filtering architecture in the testbed is the increase in loss due to the splitting and recombining process, which leads to a reduction in signal power of approximately 12.3 dB compared with using a single RF chain for each band. To counteract the losses, a second stage of amplification using another ZX60-83LN12+ LNA is placed after the combiner to maximize the received signal power while minimising the receiver NF. Each band was measured to have a gain of over 25 dB through the RF front-end.

In order to make the digital back-end of the receiver as flexible as possible, a Teledyne LeCroy WAVERUNNER 8404M-MS oscilloscope was used to implement the ADC. It has an RF bandwidth of 4 GHz, a maximum sampling rate of 40 GSample/s and a maximum resolution of 8 bit/sample, which is suitable for digitising the tri-band composite RF signal. Control of the oscilloscope is provided through National Instruments (NI) LabVIEW operating on a NI PXIe-8135 controller, connected via an Ethernet cable. This oscilloscope configuration was chosen as it has significant flexibility compared with more fixed SDR platforms, such as control over sampling rate and quantization resolution through the direct discarding of samples and bits, respectively, in LabVIEW. As such the performance of the digital back-end of the receiver with various ADC parameters, and their associated effects on processing requirements, can be explored. For the purposes of this paper, the sampling rate was fixed at 10 GSample/s, providing an oversampling rate of 3.95 for the highest carrier frequency of interest (i.e. 2.53 GHz).

The digitized RF signal is then passed to three different DDCs implemented within LabVIEW Communications Suite, also running on the PXIe controller. These use digital numerically controlled oscillators (NCOs) to downconvert each signal to BB, and perform digital filtering to extract the 20 MHz LTE signal bandwidth. The three BB waveforms are then processed using LabVIEW's LTE Application Framework (LTE-AF), obtaining the Physical Downlink Shared Channel (PDSCH) constellation and measuring its error vector magnitude (EVM). The constellation is then demodulated, obtaining transport blocks on which cyclic redundancy checks (CRCs) are performed. The CRC value indicates if a block error has been detected, which is used to calculate the channel BLER from the ratio of failed blocks to total transmitted blocks.

## III. Testbed and Simulation Model

### A. Hardware-in-the-Loop Testbed

The concurrent tri-band, direct RF sampling receiver is integrated into a Hardware-in-the-Loop (HWIL) testbed as shown in Fig. 2 in order to evaluate its performance with varying ADC resolution. For demonstration purposes, the three waveforms are all LTE downlink signals of 20 MHz bandwidth with 16-QAM modulation and 1/3 rate turbo coding, though the signals for each band could be any standard and have any bandwidth. The transmit signals are produced by the PXIe controller, with the 888 MHz band produced by LabVIEW Communications Suite's LTE-AF software and an NI-5793

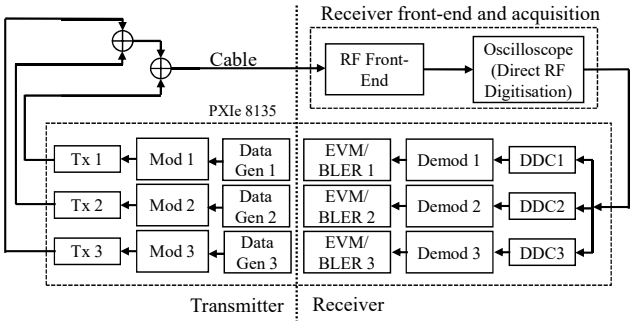


Fig. 2: Schematic block diagram of the concurrent, tri-band, direct RF sampling receiver hardware-in-the-loop testbed.

FlexRIO RF Adapter Module; whereas the 1.92 GHz and 2.53 GHz bands are produced using two NI-5791 FlexRIO RF Adapter Modules controlled by separate LabVIEW transmitters. There is no coordination or synchronization between the three signals, thereby mimicking a downlink HetNet use case. The signals from each transmitter are combined using two Mini-circuit ZAPD-2-272-S+ 2-signal combiners, and presented to the input of the receiver's RF front-end as a composite RF waveform over coaxial cable.

This paper focuses on the effect of ADC bit resolution on the multiband receiver performance when receiving three simultaneous carriers. In conventional receivers the ADC digitizes a single-band signal, which occupies the whole ADC dynamic range. However, in a multiband direct RF sampling receiver the composite signal is adjusted by automatic gain control (AGC) to occupy the ADC's dynamic range. As such, a signal in one of the bands may have significantly less power than the others, so the proportion of the dynamic range occupied by the smaller signal is reduced. For the lower power signal the ADC is desensitized as the quantization noise is effectively increased in the presence of larger signals from other bands, reducing the SNR for the low power signal. This problem, which we refer to in this paper as SNR desensitization, is a separate process from out-of-band blocking, as all bands present at the ADC's input are wanted and contain useful information, but its effects are similar. The signal power imbalance degrades the performance in the smaller signal channel, in particular, as the ADC bit resolution decreases. Finding the least ADC bit resolution to meet a target performance is, therefore, a key design parameter in multiband direct RF sampling receivers.

To explore this effect, the 1.92 GHz and 2.52 GHz bands were held at a receive power of $-50$ dBm while the received power of the 888 MHz band was varied, and its EVM and BLER measured. This is an adaptation of the adjacent channel selectivity test in the 3GPP LTE standard [12], where the 95% throughput point of a receiver, in the presence of a neighbouring signal with 39 dB more power than the desired signal's reference sensitivity level, should degrade by a maximum of 14 dB. Previous work has established that at 8 bit/sample ADC resolution, the multiband receiver experiences only 3 dB

degradation [11]. As such, the receiver should be considered 3GPP compliant for this test at any ADC resolution with up to 11 dB further degradation from the 8 bit/sample point. This aids design decisions on how complex ADCs can be while maintaining acceptable receiver performance aimed at reducing receiver power consumption.

### B. Simulation Model

To validate the measured EVM and BLER performance of the multiband direct RF sampling receiver, a computer simulation of the testbed was developed in MATLAB SIMULINK. A schematic of the modeling approach developed is illustrated in Fig. 3, which represents the functionality of the receiver architecture shown in Fig. 1. The model generates three distinct LTE BB PDSCH signals using 16QAM modulation and 1/3 rate turbo coding. Each BB signal is digitally up-converted (DUC) to one of the three carrier frequencies used in the HWIL testbed. To manage the computational complexity of the simulation model, the three RF signals are first processed individually by projecting the LNA, splitter, BPFs, and combiner effects into three equivalent RF paths, which represent the separate bandpass filtering branches of the RF front-end. The RF gains, losses and noise characteristics of the LNA, splitter, BPFs and combiner are based on the manufacturers' scattering parameters and noise figures for these components as used in the HWIL testbed.

To model the thermal noise produced by the LNA, three independent additive white Gaussian noise (AWGN) sources, each with a noise equivalent temperature of 270 K, inject noise signals into each RF path. The three processed RF signals are then added to form a composite RF signal before being amplified by a second stage of amplification (see Amp in Fig. 3), which compensates for the splitter and combiner losses. The thermal noise produced by this second amplifier is also modeled by an AWGN source with a noise equivalent temperature of 270 K. As in the tesbed, the transfer function of the second stage amplifier is realized with the same scattering parameters as the LNA. The amplified composite RF signal is then passed to the ADC for direct sampling and digitization.

Commensurate with the measurement oscilloscope used, the ADC is modelled as a 4 GHz low-pass filter followed by an ideal $n$-bit quantizer. The quantized signal is passed to three separate digital down conversion (DDC) blocks, which down convert and lowpass filter each signal to baseband. Each of the three digital streams is processed by a separate BB LTE receiver block, which outputs the constellation symbols and a CRC check for each transport block processed. The received constellation symbols are used to determine the EVM whereas the CRC check is used to determine the BLER. To align with the measured results, a received signal power of $-50$ dBm is considered for each of the 1.92 GHz and 2.52 GHz bands whereas the received power for the 888 MHz band is varied.

## IV. Measured and Simulated Results

### A. EVM Performance

The measured EVM of the 888 MHz band's PDSCH constellation for different ADC resolutions is shown in Fig. 4, under the test conditions described above. They are shown against the SNR at the input to the ADC, which is effectively the SNR of the RF front-end. As such, the degradation in performance captured as the resolution decreases is due to increased digital noise, which is largely quantization noise.

For 8 bit/sample to 6 bit/sample, there is little to no change in the EVM measured, which decreases as expected with increasing SNR to a floor of approximately 7%, which is comfortably below the 12.5% required for acceptable 16QAM performance in LTE. The minimal degradation suggests that RF noise dominates the performance up to 6 bit/sample. For the cabled testbed configuration used, this observation is commensurate with the high levels of RF noise generated by the testbed transmitters in contrast to over-the-air-measurements, which involve finite bandwidth antennas. Moving to 5 bit/sample introduces a SNR penalty of 2 dB, with EVM reaching the 12.5% mark at approximately 23 dB SNR, while 4 bit/sample intersects this point at 27 dB and 3 bit/sample at 33 dB. This represents the increasing effect of digital noise, in particular quantization noise, on performance, which in a single-band receiver is predicted to increase by 6 dB for each bit of resolution lost [14], [15].

Simulation results of EVM for the 888 MHz band are presented in Fig. 5 when the ADC resolution is varied from 8 to 4 bit/sample. A similar trend is observed to the measured results in Fig. 4. However, as the simulated results do not include the cabled transmitter noise effect, the simulated EVM performance for 8 to 6 bit/sample are more distinguishable while achieving lower EVMs at 8 and 7 bit/sample compared to measured EVMs. Simulated EVM performances for 16QAM cross the 12.5% target for 8, 7, 6, 5 and 4 bit/sample at SNR values of approximately 16, 17, 20, 24 and 30 dB, respectively.

### B. BLER Performance

Similar trends are shown in the measured BLER performance for the 888 MHz band (Fig. 6), with degradation over the 8 bit/sample case increasing from 3 dB at 5 bit/sample, through 6 dB at 4 bit/sample and finally 12 dB at 3 bit/sample. Note that the BLER reduces at a higher EVM than expected due to the use of 1/3 rate turbo coding, allowing a BLER below $10^{-2}$ at around 30% EVM when considered from an overall system perspective.

The measured BLER can then be used to calculate the effective throughput of the system (Fig. 7). With 16QAM and 1/3 rate coding the peak throughput is 15.84 Mbit/s, which assumes that blocks in error are resent. Note that performance could be improved by using LTE's hybrid automatic repeat request (HARQ) protocol, but this is left for future work. The 95% throughput point is also shown in Fig. 7, and shows that this point is reached at around 10 dB for 8 bit/sample and 7

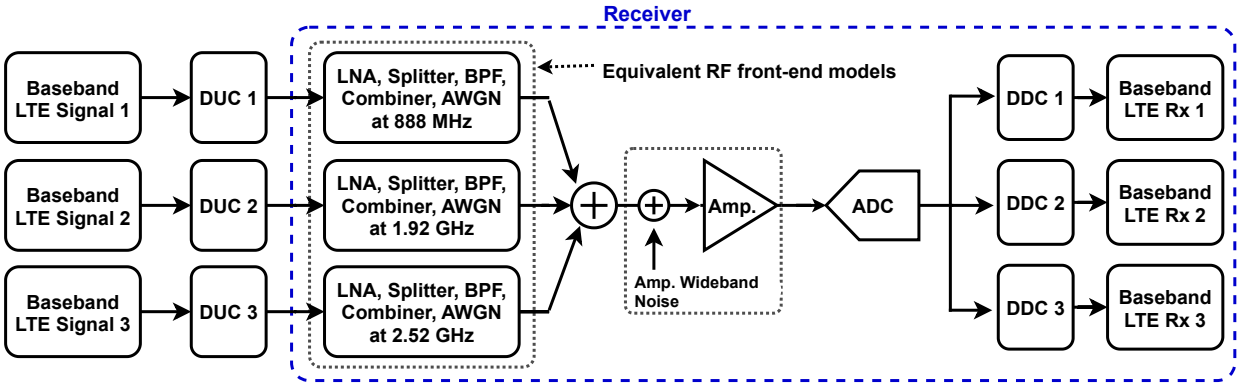


Fig. 3: Simulation model of the tri-band, direct RF sampling receiver based on the architecture in Fig. 1.

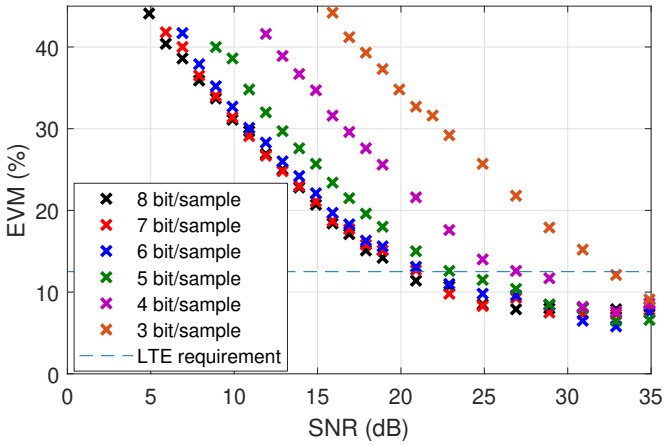


Fig. 4: Measured EVM against SNR at the ADC input, under concurrent reception conditions

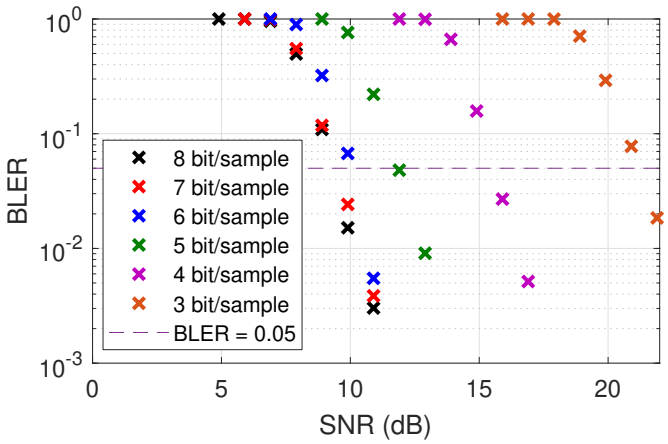


Fig. 6: Measured BLER against SNR at the ADC input, under concurrent reception conditions

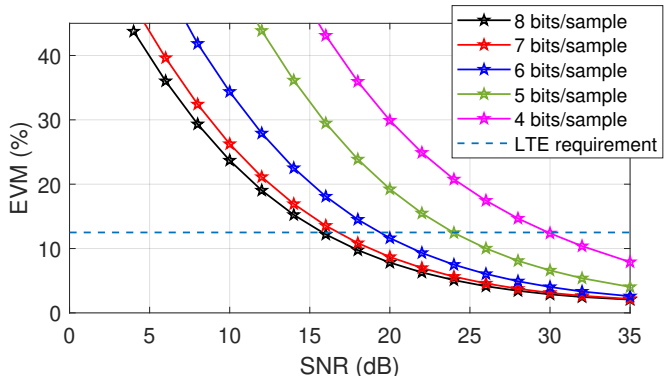


Fig. 5: Simulated EVM versus SNR at the ADC input, under concurrent reception conditions.

bit/sample. Knowing from previous work [11] that there is a 3 dB degradation from single-band to multiband reception with signals in the other two bands set at $-50$ dBm, the lowest ADC bit resolution that meets the 14 dB degradation limit in the LTE standard is 4 bit/sample, reaching 95% throughput with 9 dB greater SNR than the single-band case. The 3 bit/sample case is only just outside this reference, with a combined degradation of 15 dB. As such, the measured results demonstrate that the processing power required can be reduced significantly in multiband, direct RF sampling receivers by reducing the ADC resolution while remaining 3GPP compliant.

Simulated BLER performance versus SNR is illustrated in Fig. 8 for 6, 5, 4 and 3 bit/sample ADC resolutions. Each BLER point corresponds to counting at least 20 transport block errors, thereby achieving sufficient statistical convergence. Again, the simulated results show a similar trend to the measured BLERs in Fig. 6. At a BLER of $5 \times 10^{-2}$, which corresponds to a target throughput of 95%, achieved SNRs of 6.0, 10.4, 14.0 and 17.6 dB corresponding to 6, 5, 4 and 3 bit/sample resolutions, respectively, are obtained. This compares with 10.0, 12.0, 15.5 and 21.0 dB, respectively, for the measured results. Comparing measured and simulated results, the SNR desensitization going from 5 to 4 bit/sample resolution are approximately the same at about 3.5 dB. However, when going from 6 to 5 bit/sample resolution, the amount of SNR desensitization in the measured results is smaller. The compression of SNR desensitization in the measured results for resolutions greater than 5 bit/sample is

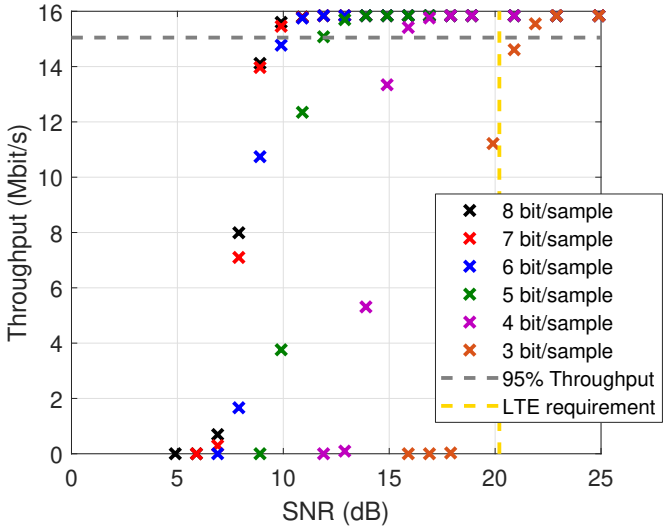


Fig. 7: Measured throughput against SNR at the ADC input, under concurrent reception conditions

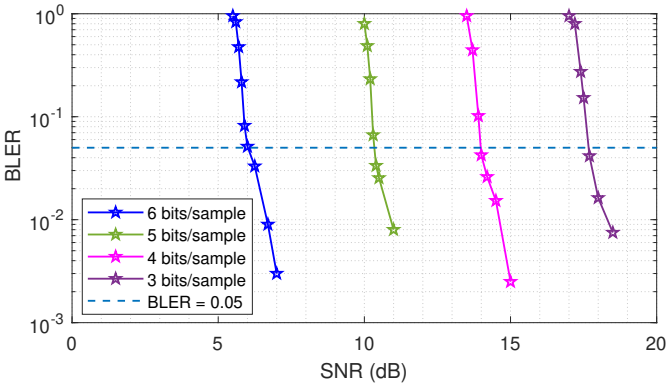


Fig. 8: Simulated BLER versus SNR at the ADC input, under concurrent reception conditions.

attributed to additional RF noise from the cabled transmitters in the testbed.

## V. Conclusions

In this paper, the EVM and BLER performance of a concurrent tri-band direct RF sampling receiver has been evaluated as a function of the ADC resolution. A HetNet interference scenario consisting of three frequency bands at 888 MHz, 1.92 GHz and 2.52 GHz has been considered. Measured performance has been obtained based on a HWIL testbed with the results verified by simulation of the system under test. In an adaptation of the adjacent channel selectivity test in the 3GPP LTE standard [12], the lowest ADC resolution that meets the allowed 14 dB degradation limit in LTE is 4 bit/sample, reaching 95% throughput with a 9 dB SNR desensitization compared to the single-band receiver. The results demonstrate that there is considerable scope for trading receiver sensitivity with ADC bit resolution, which provides an extra degree of freedom for designing low cost, low complexity and low power multiband direct RF sampling receivers for mobile broadband applications.

Acknowledgements: The authors are grateful to the UK Engineering and Physical Sciences Research Council (EPSRC) for funding to support this work under project EP/S008101/1.

## References

[1] "NR intra band Carrier Aggregation (CA) Rel-16 for xCC Down Link (DL) / yCC Up Link (UL) including contiguous and non-contiguous spectrum (x $\geq$ y)," 3GPP, Tech. Rep. 38.716-01-01, 2020, release 16.

[2] L. Sundström, M. Anderson, R. Strandberg, S. Ek, J. Svensson, F. Mu, T. Olsson, I. u. Din, L. Wilhelmsson, D. Eckerbert, and S. Mattisson, "A receiver for LTE Rel-11 and beyond supporting non-contiguous carrier aggregation," in *2013 IEEE International Solid-State Circuits Conference Digest of Technical Papers*, 2013, pp. 336–337.

[3] R. Chen and H. Hashemi, "Reconfigurable receiver with radio-frequency current-mode complex signal processing supporting carrier aggregation," *IEEE Journal of Solid-State Circuits*, vol. 50, no. 12, pp. 3032–3046, 2015.

[4] Y. Kim, J. Han, J.-S. Lee, T. Jin, P. Jang, H. Shin, J. Lee, and T. B. Cho, "Power-efficient CMOS cellular RF receivers for carrier aggregation according to RF front-end configuration," *IEEE Transactions on Microwave Theory and Techniques*, vol. 69, no. 1, pp. 452–468, 2021.

[5] R. Barrak, A. Ghazel, and F. Ghannouchi, "Optimized multistandard rf subsampling receiver architecture," *IEEE Transactions on Wireless Communications*, vol. 8, no. 6, pp. 2901–2909, 2009.

[6] J. Thabet, R. Barrak, and A. Ghazel, "Enhancement of bandpass sampling efficiency in direct rf subsampling receivers: application to multiband gps subsampling receiver," in *2014 International Conference on Multimedia Computing and Systems (ICMCS)*, 2014, pp. 1412–1417.

[7] R. H. Walden, "Analog-to-digital converter survey and analysis," *IEEE Journal on selected areas in communications*, vol. 17, no. 4, pp. 539–550, 1999.

[8] R. Barrak, A. Othman, G. I. Abib, M. Muller, M. Mabrouk, and A. Ghazel, "Design of a tunable anti-aliasing filter for multistandard RF subsampling GNSS receivers," *IEEE Transactions on Circuits and Systems II: Express Briefs*, vol. 66, no. 2, pp. 207–211, 2019.

[9] A. Rügamer, J. R. van der Merwe, I. Cortes, and W. Felber, "Theoretical and practical evaluation of an overlay multi-band front-end," in *2020 IEEE/ION Position, Location and Navigation Symposium (PLANS)*, 2020, pp. 1160–1167.

[10] D. Siafarikas and J. L. Volakis, "Toward direct RF sampling: Implications for digital communications," *IEEE Microwave Magazine*, vol. 21, no. 9, pp. 43–52, 2020.

[11] S. Henthorn, T. O'Farrell, S. Asif, M. Anbiyaei, and K. L. Ford, "Tri-band single chain radio receiver for concurrent radio," in *2020 2nd 6G Wireless Summit (6G SUMMIT)*. IEEE, 2020, pp. 1–5.

[12] "LTE; Evolved Universal Terrestrial Radio Access (E-UTRA); User Equipment (UE) conformance specification; Radio transmission and reception; Part 1: Conformance testing (3GPP TS 36.521-1 version 12.3.0 Release 12)," 3GPP, Standard, 2014.

[13] Q. Bai, R. Singh, K. L. Ford, T. O'Farrell, and R. J. Langley, "An independently tunable tri-band antenna design for concurrent multiband single chain radio receivers," *IEEE Transactions on Antennas and Propagation*, vol. 65, no. 12, pp. 6290–6297, 2017.

[14] K. K. Wong and T. O'Farrell, "Coverage of 802.11g wlans in the presence of bluetooth interference," in *14th IEEE Proceedings on Personal, Indoor and Mobile Radio Communications, 2003. PIMRC 2003.*, vol. 3, 2003, pp. 2027–2031.

[15] Q. Gu, *RF system design of transceivers for wireless communications*. Springer Science & Business Media, 2006.